J|A|C|S ARTICLES

Published on Web 05/12/2010

Total Synthesis and Biological Evaluation of the Resveratrol-Derived Polyphenol Natural Products Hopeanol and Hopeahainol A

K. C. Nicolaou,* Qiang Kang, T. Robert Wu, Chek Shik Lim, and David Y.-K. Chen*

Chemical Synthesis Laboratory at Biopolis, Institute of Chemical and Engineering Sciences (ICES), Agency for Science, Technology and Research (ASTAR), 11 Biopolis Way, The Helios Block, 03-08, Singapore 138667

Received March 29, 2010; E-mail: kcn@scripps.edu; david_chen@ices.a-star.edu.sg

Abstract: The total synthesis and biological evaluation of the resveratrol-derived natural products hopeanol (**2**) and hopeahainol A (**3**) in their racemic and antipodal forms are described. The Friedel−Crafts-based synthetic strategy employed was developed from model studies that established the feasibility of constructing the C_{7b} quaternary center through an intramolecular Friedel−Crafts reaction and a Grob-type fragmentation to introduce an obligatory olefinic bond in the growing molecule. The final stages of the synthesis involved an epoxide substrate and an intramolecular Friedel−Crafts reaction, followed by oxidation to afford, upon global deprotection, hopeahainol A (**3**). The latter was converted under basic conditions to hopeanol (**2**), whereas the reverse transformation, previously suggested as a step in the biosynthesis of hopeahainol A (**3**), was not observed under a variety of conditions. Biological evaluation of the synthesized compounds confirmed the reported acetylcholinesterase inhibitory activity of hopeahainol A (**3**) but not the reported cytotoxic potencies of hopeanol (**2**).

Introduction

The polyphenolic natural products represent a large and growing class of structurally diverse compounds exhibiting a wide range of biological activities.[1] Despite of the large membership of this resveratrol-derived collection of secondary metabolites, most of the attention has focused primarily on the parent compound, resveratrol (**1**, Figure 1), for which a variety of potentially useful properties have been demonstrated. These include anti-inflammatory,[2] antiaging,[3] antitumor,[4] cardiovascular,[5] and neuroprotective[6] properties in both *in vitro* and *in vivo* assays. Taken together with its substantial concentration in red wine (∼3−5 mg in a 750 mL bottle), this biological profile gave support for the so-called "French Paradox", the idea that a balanced consumption of red wine may neutralize the harmful nutritional effects of foods high in fat and cholesterol.[7] The increasing interest in the resveratrol-derived polyphenol natural products is appropriately reflected in the recent spate of

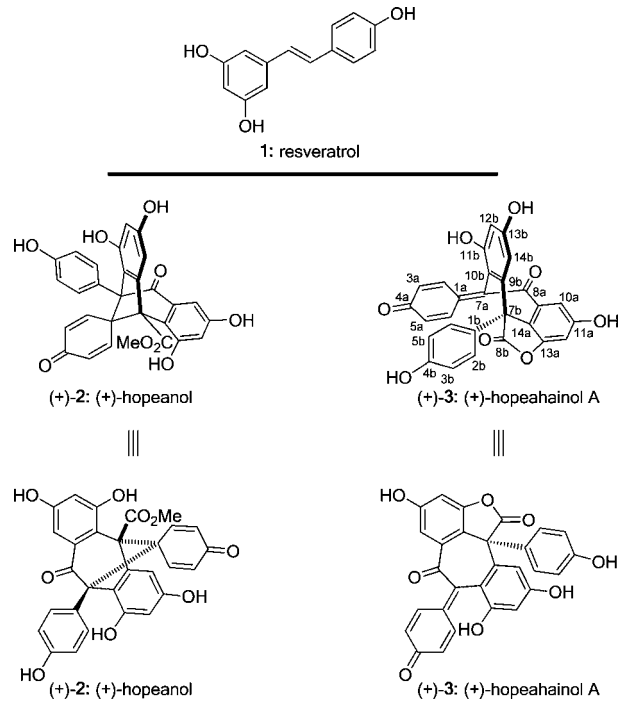

Figure 1. Molecular structures of resveratrol (**1**), (+)-hopeanol [(+)-**2**], and hopeahainol A [(+)-**3**].

(1) For representative reviews on the chemical and biological studies of natural polyphenols, see: (a) Yang, C. S.; Lambert, J. D.; Sang, S. *Arch. Toxicol.* **2009**, *83*, 11–21. (b) Bonfili, L.; Cecarini, V.; Amici, M.; Cuccioloni, M.; Angeletti, M.; Keller, J. N.; Eleuteri, A. M. *FEBS J.* **2008**, *275*, 5512–5526. (c) Habauzit, V.; Horcajada, M.-N. *Phytochem. Rev.* **2008**, *7*, 313–344. (d) Lafay, S.; Gil-Izquierdo, A. *Phytochem. Rev.* **2008**, *7*, 301–311. (e) Halliwell, B. *Arch. Biochem. Biophys.* **2008**, *476*, 107–112. (f) Korkina, L. G.; Pastore, S.; De Luca, C.; Kostyuk, V. A. *Curr. Drug Metab.* **2008**, *9*, 710–729, and references cited within.

(2) (a) Udenigwe, C. C.; Ramprasath, V. R.; Aluko, R. E.; Jones, P. J. *Nutr. Rev.* **2008**, *66*, 445–454. (b) Shapiro, H.; Singer, P.; Halpern, Z.; Bruck, R. *Gut* **2007**, *56*, 426–435. (c) Lastra, D.; Catalina, A.; Villegas, I. *Mol. Nutr. Food Res.* **2005**, *49*, 405–430.

(3) (a) Bertelli, A. A. A.; Das, D. K. *J. Cardiovasc. Pharmacol.* **2009**, *54*, 468–476. (b) Das, D. K.; Maulik, N. *Mol. Interv.* **2006**, *6*, 36–47. (c) Olas, B.; Wachowicz, B. *Platelets* **2005**, *16*, 251–260. (d) Bradamante, S.; Barenghi, L.; Villa, A. *Cardiovasc. Drug Rev.* **2004**, *22*, 169–188. (e) Fremont, L. *Life Sci.* **2000**, *66*, 663–673.

(4) (a) Valenzano, D. R.; Cellerino, A. *Cell Cycle* **2006**, *5*, 1027–1032. (b) de la Lastra, C. A.; Villegas, I. *Mol. Nutr. Food Res.* **2005**, *49*, 405–430. (c) Brisdelli, F.; D'Andrea, G.; Bozzi, A. *Curr. Drug Metab.* **2009**, *10*, 530–546.

 10.1021/ja102623j

reports, notably from the Snyder group,[8] describing the total syntheses of natural products belonging to this class.

In 2006, Tan and co-workers disclosed the structural elucidation and cytotoxic properties ($IC_{50} = 0.52-19.36\ \mu M$) against a panel of selected cancer cell lines (KB, AGS, Hela, BEL-7402, SW1116, and BGC-803) of hopeanol (**2**, Figure 1), a polyphenol secondary metabolite isolated from the bark of *Hopea exalata*.[9] A subsequent investigation of *H. hainanensis* led to, in addition to hopeanol (**2**), the isolation of the structurally related hopeahainol A (**3**, Figure 1).[10] The latter exhibited inhibitory activity against acetylcholinesterase ($IC_{50} = 4.33\ \mu M$), an enzyme implicated and exploited for the treatment of Alzheimer's disease.[10] A radical-based biosynthetic hypothesis has been put forward by the isolation chemists for the biosynthesis of hopeanol (**2**) and hopeahainol A (**3**) from resveratrol (**1**) that postulated the former (i.e., **2**) as the precursor of the latter (i.e., **3**).[10] In 2009, we reported[11] the first total synthesis of hopeanol (**2**) and hopeahainol A (**3**) in their racemic forms through a short and efficient route involving a series of cascade reactions[12] and novel skeletal rearrangements. In this article, we provide the full account of our studies in this area, including the enantioselective total synthesis of both enantiomeric forms of **2** and **3**, and biological evaluation of selected synthesized compounds.

Results and Discussion

Below we lay out the details of these investigations as they evolved, beginning from the initial considerations of a synthetic strategy toward hopeanol (**2**) and hopeahainol A (**3**) and ending with the biological evaluation of selected synthesized compounds.

Retrosynthetic Analysis. Our final synthetic strategy toward hopeanol (**2**) and hopeahainol A (**3**), as presented in Figure 2

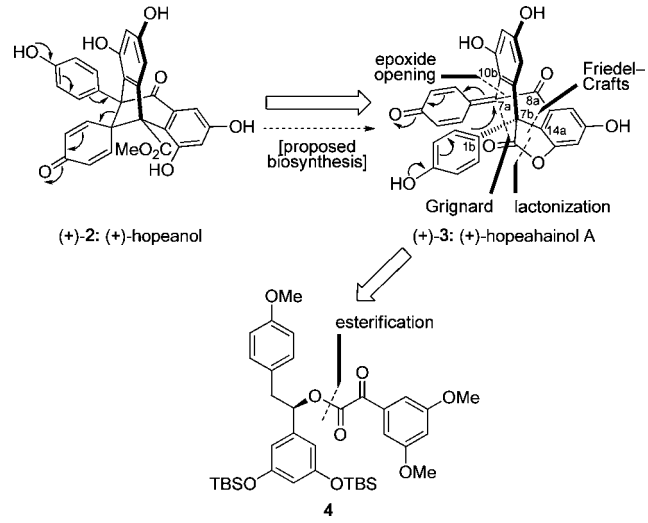

Figure 2. Final synthetic strategy toward (+)-hopeahainol A [(+)-**3**], and (+)-hopeanol [(+)-**2**] shown in retrosynthetic format. TBS = *tert*-butyldimethyl silyl.

in retrosynthetic format, was derived from a number of model studies which will be described below. Thus, the key reactions for the assembly of the hopeahainol A structure were a lactonization, a Grignard reaction ($C_{1b}-C_{7b}$ bond), an intramolecular Friedel–Crafts-type[13] reaction ($C_{7b}-C_{14a}$ bond), and an intramolecular epoxide opening ($C_{7a}-C_{10b}$ bond, C_{8a} oxygen) (see Figure 2, structure **3**). Its proposed conversion to hopeanol (**3** → **2**, Figure 2) runs counter to the proposed biosynthetic hypothesis[10] which postulated the reverse transformation (**2** → **3**, Figure 2), although at the outset both interconversions were considered plausible. Central to the successful strategy was the stepwise construction of the C_{7b} quaternary stereocenter, residing at the heart of the structure, starting from ketoester **4** (Figure 2), whose origin from the corresponding hydroxyl and carboxylate components was obvious.

Model Studies for the Construction of the Quaternary Center (C_{7b}) of Hopeahainol A and Hopeanol. Our designed model studies were intended to explore methods for building the quaternary center of hopeahainol A (**3**) and hopeanol (**2**) with appropriate appendages. In our first foray (see Scheme 1a), we targeted the simple triaryl methyl ester **12** through an intermolecular Friedel–Crafts-type reaction involving tertiary alcohol **9** as the main substrate and phenol (**11**) as the external nucleophile. Thus, sequential addition of Grignard reagents **6** and **8** to dimethyl oxalate (**5**) furnished tertiary alcohol methyl ester **9**, through ketoester **7**, in 66% overall yield (based on **5**). Pleasantly, exposure of a solution of tertiary alcohol **9** and phenol (**11**) in CH_2Cl_2 to an excess *p*-TsOH·H_2O (23 → 40 °C) led to the formation of the desired product **12** in excellent yield (97%), presumably through the intermediacy of carbocation **10** as shown in Scheme 1a.

Encouraged by this initial result, we proceeded to test the feasibility of synthesizing the more relevant and advanced model system **18** as shown in Scheme 1b. In this instance, the desired

(5) (a) Bastianetto, S.; Dumont, Y.; Han, Y.; Quirion, R. *CNS Neurosci. Ther.* **2009**, *15*, 76–83. (b) Raval, A. P.; Lin, H. W.; Dave, K. R.; DeFazio, R. A.; Della Morte, D.; Kim, E. J.; Perez-Pinzon, M. A. *Curr. Med. Chem.* **2008**, *15*, 1545–1551. (c) Spasic, M. R.; Callaerts, P.; Norga, K. K. *Neuroscientist* **2009**, *15*, 309–316. (d) Sun, A. Y.; Wang, Q.; Simonyi, A.; Sun, G. Y. *Neuromol. Med.* **2008**, *10*, 259–274.

(6) (a) Delmas, D.; Lancon, A.; Colin, D.; Jannin, B.; Latruffe, N. *Curr. Drug Targets* **2006**, *7*, 423–442. (b) Kraft, T. E.; Parisotto, D.; Schempp, C.; Efferth, T. *Crit. Rev. Food Sci. Nutr.* **2009**, *49*, 782–799. (c) Shakibaei, M.; Harikumar, K. B.; Aggarwal, B. B. *Mol. Nutr. Food Res.* **2009**, *53*, 115–128. (d) Chillemi, R.; Sciuto, S.; Spatafora, C.; Tringali, C. *Nat. Prod. Commun.* **2007**, *2*, 499–513. (e) Garg, A. K.; Buchholz, T. A.; Aggarwal, B. B. *Antioxid. Redox Signaling* **2005**, *7*, 1630–1647. (f) Aggarwal, B. B.; Bhardwaj, A.; Aggarwal, R. S.; Seeram, N. P.; Shishodia, S.; Takada, Y. *Anticancer Res.* **2004**, *24*, 2783–2840.

(7) For reviews, see: (a) Saiko, P.; Szakmary, A.; Jaeger, W.; Szekeres, T. *Rev. Mutat. Res.* **2007**, *658*, 68–94. (b) Walle, T.; Hsieh, F.; DeLegge, M. H.; Oatis, J. E.; Walle, U. K. *Drug Metab. Dispos.* **2004**, *32*, 1377–1382. (c) Athar, M.; Back, J. H.; Tang, X.; Kim, K. H.; Kopelovich, L.; Bickers, D. R.; Kim, A. L. *Toxicol. Appl. Pharmacol.* **2007**, *224*, 274–278. (d) Soleas, G. J.; Diamandis, E. P.; Goldberg, D. M. *Clin. Biochem.* **1997**, *30*, 91–113. (e) Kopp, P. *Eur. J. Endocrinol.* **1998**, *138*, 619–620.

(8) (a) Snyder, S. A.; Breazzano, S. P.; Ross, A. G.; Lin, Y.; Zografos, A. L. *J. Am. Chem. Soc.* **2009**, *131*, 1753–1765. (b) Snyder, S. A.; Zografos, L.; Lin, Y. *Angew. Chem., Int. Ed.* **2007**, *46*, 8186–8191.

(9) Ge, H. M.; Xu, C.; Wang, X. T.; Huang, B.; Tan, R. X. *Eur. J. Org. Chem.* **2006**, 5551–5554.

(10) Ge, H. M.; Zhu, C. H.; Shi, D. H.; Zhang, L. D.; Xie, D. Q.; Yang, J.; Ng, S. W.; Tan, R. X. *Chem.—Eur. J.* **2008**, *14*, 376–381.

(11) Nicolaou, K. C.; Wu, R. T.; Kang, Q.; Chen, D. Y.-K. *Angew. Chem., Int. Ed.* **2009**, *48*, 3340–3343.

(12) (a) Nicolaou, K. C.; Montagnon, T.; Snyder, S. A. *Chem. Commun.* **2003**, *5*, 551–564. (b) Tietze, L. F.; Brasche, G.; Gericke, K. M. *Domino Reactions in Organic Synthesis*; Wiley-VCH: Weinheim, 2006. (c) Nicolaou, K. C.; Edmonds, D. J.; Bulger, P. G. *Angew. Chem., Int. Ed.* **2006**, *45*, 7134–7186.

(13) For reviews, see: (a) Olah, G. A. *Friedel-Crafts and Related Reactions*; Wiley: New York, 1963. (b) Olah, G. A. *Friedel-Crafts Chemistry*; Wiley: New York, 1973. (c) Olah, G. A.; Krishnamurti, R.; Prakash, G. K. S. *Comprehensive Organic Synthesis*; Pergamon: Oxford, 1991; Vol. 3, pp 293.

(14) Corey, E. J.; Helal, C. J. *Angew. Chem., Int. Ed.* **1998**, *37*, 1986–2012.

Scheme 1. Synthesis of (a) Model Methyl Ester **12** and (b) Model γ-Lactone **18** through Intermolecular Friedel–Crafts Reactions[a]

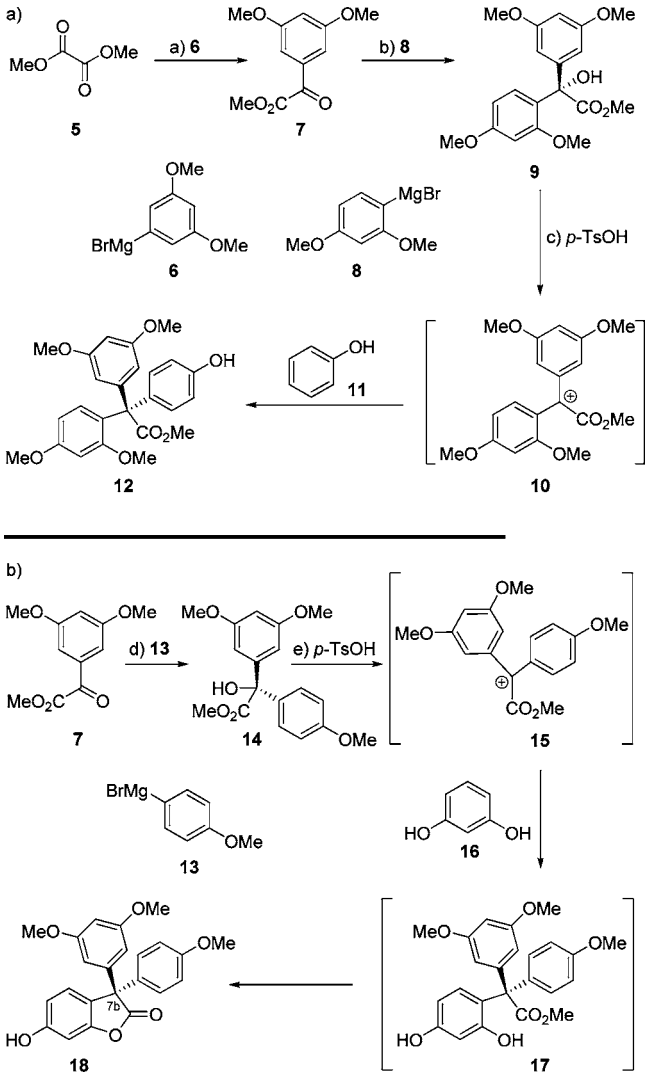

[a] Reagents and conditions: (a) dimethyl oxalate (**5**) (2.0 equiv), 3,5-dimethoxyphenylmagnesium bromide (**6**, prepared from 1-bromo-3,5-dimethoxybenzene and magnesium turnings) (1.0 M in THF, 1.0 equiv), THF, −78 °C, 0.5 h, 80%; (b) 2,4-dimethoxyphenylmagnesium bromide (**8**, prepared from 1-bromo-2,4-dimethoxybenzene and magnesium turnings) (0.23 M in THF, 1.9 equiv), THF, 0 °C, 0.5 h, 83%; (c) phenol (**11**) (3.0 equiv), *p*-TsOH·H_2O (3.0 equiv), CH_2Cl_2, 23 → 40 °C, 4 h, 97%; (d) 4-methoxyphenylmagnesium bromide (**13**, prepared from 1-bromo-4-methoxybenzene and magnesium turnings) (0.4 M in THF, 2.0 equiv), THF, 0 °C, 0.5 h, 81%; (e) resorcinol (**16**, 3.0 equiv), *p*-TsOH·H_2O (3.0 equiv), toluene, 23 → 75 °C, 20 min, 90%. *p*-TsOH = *para*-toluenesulfonic acid.

Scheme 2. Attempted Synthesis of (a) γ-Lactone **22** and (b) Methyl Ester **26** through Intermolecular Friedel–Crafts Reactions[a]

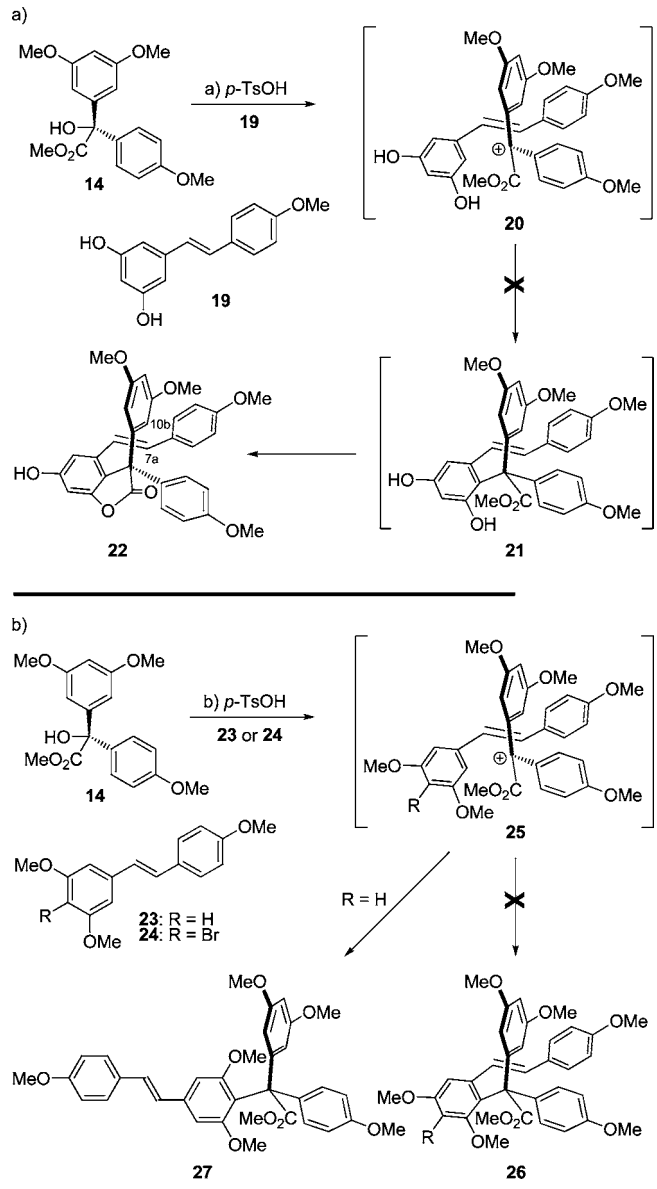

[a] Reagents and conditions: (a) **19** (3.0 equiv), *p*-TsOH·H_2O (3.0 equiv), CH_2Cl_2, 23 → 50 °C, 4 h; (b) **23** or **24** (3.0 equiv), *p*-TsOH·H_2O (3.0 equiv), CH_2Cl_2, 23 → 50 °C, 2 h, **27**:80% (from **23**).

tertiary alcohol methyl ester substrate **14** was prepared from methyl glyoxalate derivative **7** by addition of Grignard reagent **13** (81% yield). The latter underwent a smooth Friedel–Crafts-type reaction with resorcinol (**16**) under conditions similar to those in Scheme 1a (*p*-TsOH·H_2O, 23 → 75 °C) to afford the expected tetracyclic model system **18** (90% yield), presumably through transient intermediate carbocation **15** and diphenolic methyl ester **17**, the latter apparently undergoing spontaneous lactonization under the reaction conditions employed.

The successful construction of model system **18** (containing four of the six ring systems of hopeahainol A) gave impetus to our next logical step, which was to attempt to apply the developed technology to assemble the entire carbon backbone of hopeahainol A (**3**). Scheme 2 summarizes these attempts. It was anticipated that using diphenol **19** as the nucleophilic partner in the Friedel–Crafts reaction employing tertiary alcohol methyl ester **14** would enable us to obtain a product (**20** → **21** → **22**, Scheme 2a) containing five of the six rings of hopeahainol A and equipped with an olefinic bond that could serve as a handle to forge the final ring of the molecule through formation of the C_{7a}–C_{10b} bond. In the event, however, and under the previously employed conditions, neither the lactone **22** nor methyl ester **21** were observed.

In a second attempt (see Scheme 2b) to construct such an advanced intermediate (i.e., **26**), we employed protected nucleophilic partner **23**, but unfortunately, again to no avail. Instead, regioisomeric product **27** was formed in 80% yield under the previously developed conditions for the Friedel–Crafts reaction. A last-ditch attempt to avoid the latter outcome by employing bromide **24**, where the bromine residue was expected

Scheme 3. Synthesis of Lactone **33** through Intramolecular Friedel−Crafts Reaction[a]

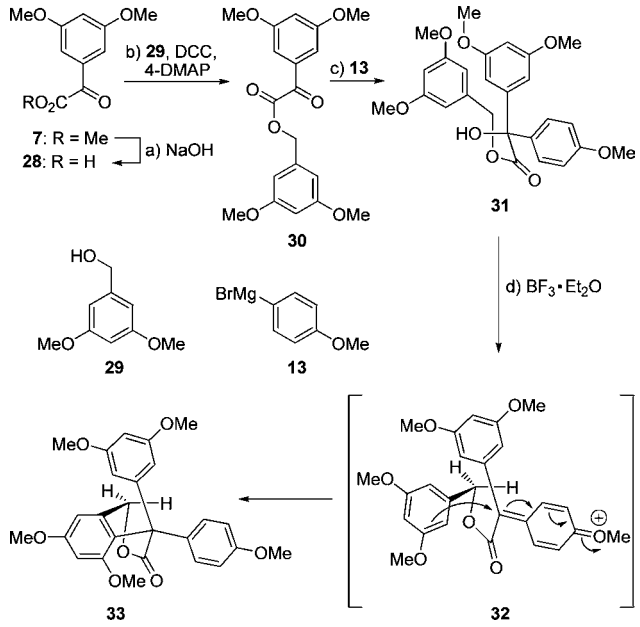

[a] Reagents and conditions: (a) THF/NaOH (2.0 N aq) (1:1), 23 °C, 0.5 h, 98%; (b) **28** (1.5 equiv), **29** (1.0 equiv), DCC (3.0 equiv), 4-DMAP (0.3 equiv), CH_2Cl_2, 23 °C, 12 h, 85%; (c) 4-methoxyphenylmagnesium bromide (**13**, prepared from 1-bromo-4-methoxybenzene and magnesium turnings) (0.1 M in THF, 1.8 equiv), THF, −10 °C, 5 min, 81%; (d) $BF_3 \cdot Et_2O$ (3.0 equiv), CH_2Cl_2, 0 °C, 2 h, 86%. DCC = dicyclohexylcarbodiimide, 4-DMAP = 4-dimethylaminopyridine.

to block the undesired pathway, also failed, leading to a complex mixture of unwanted materials.

Having failed to apply the developed intermolecular Friedel−Crafts-based sequence to an advanced intermediate toward hopeahainol A, and recognizing the factors responsible for these failures, we decided to explore the intramolecular version of this venerable reaction in order to accomplish this task. We reasoned that by tethering the two partners and postponing the introduction of the desired olefinic bond until after the Friedel−Crafts reaction, we could perhaps avoid the pitfalls encountered in the intermolecular version of the process, namely the wrong regioselectivity (by virtue of enforced proximity) and the interference from the olefinic bond (by virtue of its absence). To test the former hypothesis (regarding regioselection), we designed the simple model study directed toward the construction of model system **33** as summarized in Scheme 3. Thus, saponification (NaOH) of methyl glyoxalate **7**, followed by esterification of the resulting carboxylic acid (**28**) with benzylic alcohol **29** (DCC), led to α-ketoester **30** (83% overall yield). Reaction of the latter with *p*-methoxyphenyl Grignard reagent **13** furnished tertiary alcohol **31** in 81% yield. Exposure of the latter to $BF_3 \cdot Et_2O$ in CH_2Cl_2 at 0 °C resulted in the formation of the desired tetracyclic product **33** in 86% yield, presumably through intermediate **32**.

The initial success with the intramolecular Friedel−Crafts approach to model system **33** set the stage for the next advance. Thus, in an effort to include in our growing molecule all the carbon atoms needed for the synthesis of hopeahainol A, we undertook the study shown in Scheme 4. Treatment of aldehyde **34** with the lithioderivative obtained from aryl bromide **35** and *n*-BuLi, followed by esterification of the resulting alcohol (**36**) with carboxylic acid **28** (DCC), furnished α-ketoester **37** in 71% overall yield. Addition of Grignard reagent **13** to the latter gave

Scheme 4. Synthesis of Methyl Ester **42** through Intramolecular Friedel−Crafts Reaction[a]

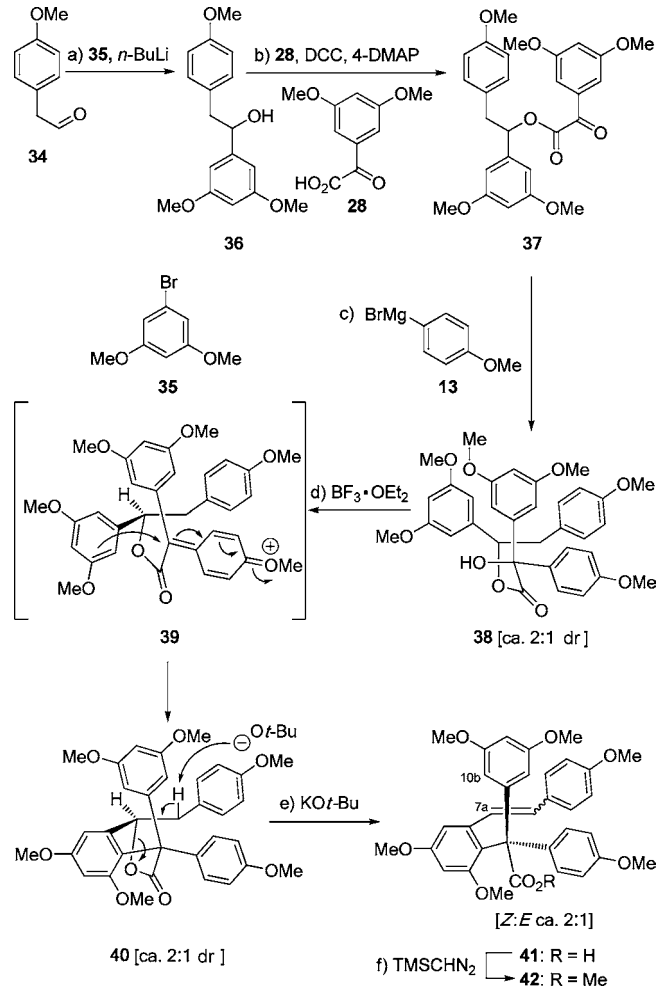

[a] Reagents and conditions: (a) **34** (1.1 equiv), **35** (1.0 equiv), *n*-BuLi (1.6 M in THF, 1.1 equiv), THF, −78 °C, 0.5 h, 75%; (b) **28** (1.5 equiv), **36** (1.0 equiv), DCC (2.0 equiv), 4-DMAP (0.1 equiv), CH_2Cl_2, 0 → 23 °C, 2 h, 95%; (c) 4-methoxyphenylmagnesium bromide (**13**, prepared from 1-bromo-4-methoxybenzene and magnesium turnings) (0.1 M in THF, 1.9 equiv), THF, 0 °C, 0.5 h, 84% (∼2:1 mixture of diastereoisomers); (d) $BF_3 \cdot Et_2O$ (2.0 equiv), CH_2Cl_2, 0 °C, 1 h, 74% (∼2:1 mixture of diastereoisomers); (e) KO*t*-Bu (5.7 equiv), THF, 0 → 23 °C, 2 h; (f) $TMSCHN_2$ (2.0 M in Et_2O, 5.7 equiv), MeOH/THF (1:1), 23 °C, 10 min, 95% for the two steps from **40** (∼2:1 mixture of *Z*/*E* stereoisomers).

tertiary alcohol **38** as a mixture of diastereoisomers (∼2:1 dr) in 84% yield. The intended cyclization proceeded under the established Lewis acid conditions ($BF_3 \cdot Et_2O$, CH_2Cl_2, 0 °C), affording the desired pentacyclic system **40** (∼2:1 dr) through the presumed intermediacy of oxocation **39** (74% yield). The unmasking of the desired olefinic bond hidden behind the lactone moiety was achieved by treatment of the latter compound with KO*t*-Bu to furnish, through a fragmentation reaction, carboxylic acid **41**, whose methylation ($TMSCHN_2$) led to olefinic methyl ester **42** (∼2:1 ratio of *Z*/*E* isomers) in 95% yield. However, attempts to complete the ring framework of hopeahainol A (formation of $C_{7a}-C_{10b}$ bond) through a second Friedel−Crafts reaction under a variety of conditions (e.g., Lewis or protic acids) failed, leading instead to decomposition and/or recovery of starting material. Under these circumstances, a new plan had to be devised.

Total Synthesis of (−)-Hopeahainol A [(−)-(3)], (−)-Hopeanol [(−)-(2)], (+)-Hopeahainol A [(+)-(3)], and (+)-Hopeanol

[(+)-(2)]. While the synthesis of advanced intermediate **42** (Scheme 4) was a significant development, the difficulties encountered in its attempted elaboration to the target molecule called for further deliberation. We hypothesized that by locking the conformation of the ultimate precursor of hopeahainol A through formation of the γ-lactone moiety present in the natural product we might facilitate the casting of the last ring. We also considered the employment of an epoxide moiety in place of the olefinic bond as the enabling handle to effect the desired carbon−carbon bond formation (C_{7a}−C_{10b}) upon suitable activation. It was with these inspiring rationales that we proceeded to the next phase of the campaign, which required first the construction of the diphenolic γ-lactone **52** and/or **53** through hydroxyester **49** (see Scheme 5). The synthesis of the latter (∼1:1 dr) proceeded along the lines delineated above for **40** (Scheme 4) with an appropriate modification as shown in Scheme 5. Thus, addition of the lithioderivative obtained from bis-TBS aryl bromide **43** to aldehyde **34** furnished, after PCC oxidation of the resulting alcohol (**44**, 75% yield), ketone **45** (99% yield). (+)-CBS reduction [(*S*)-(+)-2-methyl-CBS-oxazaborolidine, catecholborane] of the latter led to benzylic alcohol **46** in 85% yield and 96% ee (chiral HPLC analysis). Coupling of benzylic alcohol **46** with α-ketoacid **28** (DCC, 4-DMAP) gave α-ketoester **4** (95% yield), and reaction of the latter with Grignard reagent **13** led to diphenolic hydroxyester **49** after desilylation (TBAF, 79% overall yield, ∼1:1 dr) of the resulting bis-TBS product (**48**). Exposure of substrate **49** (∼1:1 dr) to $BF_3 \cdot Et_2O$ in CH_2Cl_2 at ambient temperature furnished diastereomeric products **52** and **53** (86% yield, ∼1:1.3 dr), presumably through diastereomeric transition states **50** and **51**, respectively. Since the ratio of the two products (diastereomeric at C_{7b}) would be reflected in the enantiomeric ratio of the expected downstream olefinic γ-lactones (i.e., structures *ent*-**57** and **57**, Scheme 6), we sought to optimize the diastereoselectivity of this intramolecular Friedel−Crafts reaction. Screening of a variety of Lewis and protic acids was revealing. Thus, and as shown in Table 1, a number of promoters, such as *p*-TsOH·H_2O, TFA, $Sc(OTf)_3$, and $Yb(OTf)_3$, were found to be effective (entries 7, 8, 10, and 11), with *p*-TsOH·H_2O resulting in the highest diastereoselectivity (**52**:**53** ∼1:2.4 dr) and the lanthanide Lewis acids in the highest yields (91% and 88% yield, respectively, **52**:**53** ∼1:1.5 dr). Apparently, from the two competing transition states (**50** and **51**, Scheme 5), the one leading to **53** (i.e., **51**) is energetically somewhat more stable than the one leading to **52** (i.e., **50**). Chromatographic separation of the two diastereomeric products allowed crystallization of the major compound (**53**), whose X-ray crystallographic analysis provided unambiguous confirmation of its structure, including its absolute configuration (see ORTEP, Figure 3),[15] and, thereby, that of its minor diastereoisomer (**52**).

With intermediates **52** and **53** structurally secured, their independent advancement to the corresponding olefinic γ-lactones was undertaken and successfully completed as outlined in Scheme 6. Initial attempts to apply the same conditions as previously employed for the conversion of **40** to **41** (KO*t*-Bu, see Scheme 4) led to translactonization, as evidenced by the isolation of the dihydroxy γ-lactones **54** and **55**, rather than formation of the expected olefinic product. Upon considerable experimentation, this problem was circumvented by the use of KO*t*-Bu in the presence of 18-crown-6 in THF, conditions that completely suppressed the formation of the undesired translactonization products and led to the generation of the desired

Scheme 5. Synthesis of Diastereomeric Lactones **52** and **53**[a]

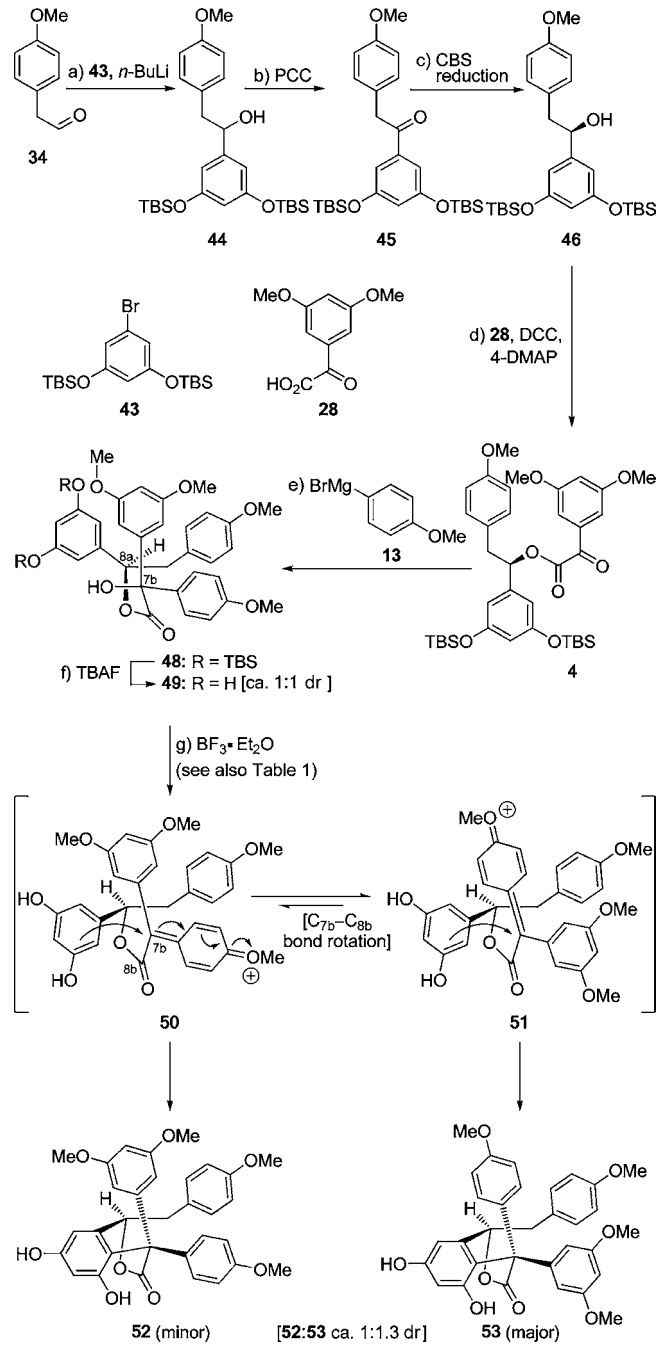

[a] Reagents and conditions: (a) **43** (1.0 equiv), **34** (1.16 equiv), *n*-BuLi (1.6 M in THF, 1.1 equiv), THF, −78 °C, 0.5 h, 75%; (b) PCC (3.0 equiv), CH_2Cl_2, 0 → 23 °C, 12 h, 99%; (c) (*S*)-(+)-2-methyl-CBS-oxazaborolidine (0.2 equiv), catecholborane (1.0 equiv), toluene, 0 °C, 0.5 h, 85% (96% ee as determined by chiral HPLC); (d) **28** (1.5 equiv), **46** (1.0 equiv), DCC (2.3 equiv), 4-DMAP (0.3 equiv), CH_2Cl_2, 23 °C, 12 h, 95%; (e) 4-methoxyphenylmagnesium bromide (**13**, prepared from 1-bromo-4-methoxybenzene and magnesium turnings) (0.26 M in THF, 1.3 equiv), THF, −10 °C, 0.5 h; (f) TBAF (1.0 M in THF, 2.0 equiv), THF, 0 °C, 0.5 h, 79% for the two steps from **4** (∼1:1 mixture of diastereoisomers); (g) $BF_3 \cdot Et_2O$ (3.0 equiv), CH_2Cl_2, 23 °C, 4 h, 86% (**52**:**53** ∼1:1.3 dr) (see also Table 1). PCC = pyridinium chlorochromate, TBAF = tetra-*n*-butylammonium fluoride.

(15) CCDC-769640 contains the supplementary crystallographic data for compound **53**. This data can be obtained free of charge from The Cambridge Crystallographic Data Centre via www.ccdc.cam.ac.uk/data_request/cif.

Scheme 6. Synthesis of Lactones *ent*-**58** and **58**[a]

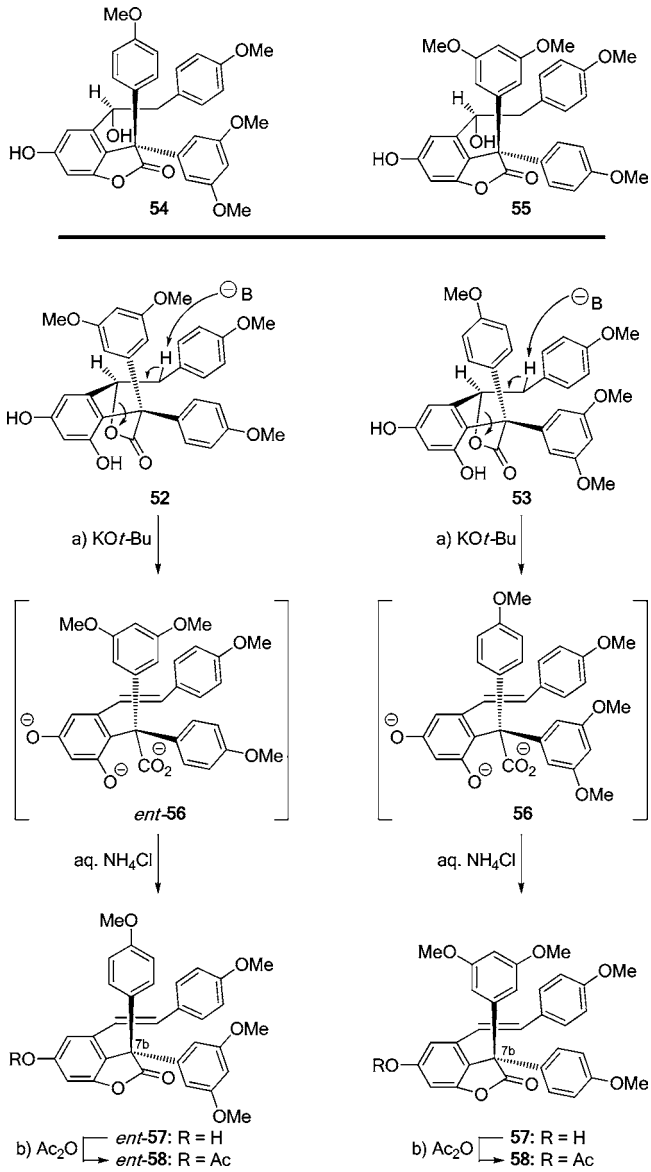

[a] Reagents and conditions: (a) **52** or **53**, KO*t*-Bu (10.0 equiv), 18-crown-6 (11 equiv), THF, 0 → 23 °C, 20 h, *ent*-**57**:72% or **57**:78%; (b) Ac_2O (1.4 equiv), 4-DMAP (0.1 equiv), pyridine, 0 → 23 °C, 1 h, 100%. Ac = acetyl.

Table 1. Intramolecular Friedel−Crafts Reaction of Tertiary Alcohol **49** Leading to Pentacyclic Lactones **52** and **53**[a]

entry	promoter	conversion (%)[b]	time (h)	yield (%)[c]	**52:53** (ratio)
1	$BF_3 \cdot Et_2O$	100	4	86	1:1.3
2	$TiCl_4$	100	2	0[d]	–
3	$Ti(Oi\text{-}Pr)_4$	100	2	0[d]	–
4	$AlCl_3$	100	4	trace[e]	1:1
5	Me_2AlCl	100	4	0[d]	–
6	$ZnCl_2$	0	12	0[f]	–
7	*p*-TsOH·H_2O	100	12	65	1:2.4
8	TFA	100	12	85	1:1.2
9	$CeCl_3$	0	12	0[f]	–
10	$Sc(OTf)_3$	100	12	91	1:1.5
11	$Yb(OTf)_3$	100	12	88	1:1.5

[a] Reactions were carried out under the following conditions: **49** (0.1 mmol), promoter (3.0 equiv), CH_2Cl_2 (3.0 mL), 23 °C. [b] Based on crude ^1H NMR spectroscopic analysis. [c] Yields refer to chromatographically and spectroscopically homogeneous materials. [d] Decomposition was observed. [e] Based on crude ^1H NMR spectroscopic analysis. [f] Starting material recovered.

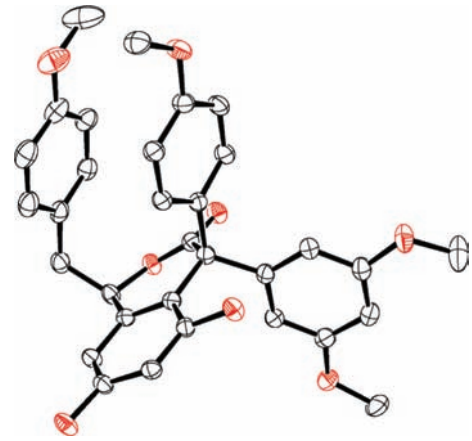

Figure 3. X-ray-derived ORTEP of lactone **53** with thermal ellipsoids shown at the 50% probability level.[15]

olefinic γ-lactones *ent*-**57** (72% yield, from **52**) and **57** (78% yield from **53**) after quenching with aq NH_4Cl. These reactions presumably proceed through trianion intermediates *ent*-**56** and **56**, respectively. Compounds *ent*-**57** and **57** were converted to their acetate derivatives (*ent*-**58** and **58**, respectively) under standard conditions (Ac_2O, 4-DMAP, py) in quantitative yields.

At this juncture we chose the major enantiomer **58** (Scheme 6) for further elaboration due to its abundance, even though it was destined to yield (−)-hopeahainol A [(−)-**3**], rather than the natural enantiomeric form of (+)-hopeahainol A [(+)-**3**]. We, of course, planned to return to the minor enantiomer *ent*-**58** for its elaboration to the natural product once the final stages of the route had been worked out, or even backtrack to the CBS reduction step to obtain the opposite enantiomer of benzylic alcohol **46** (i.e., *ent*-**46**, see Scheme 5), which would lead us to the correct diastereoisomer *ent*-**58** as the major product, thereby resulting in an enantioselective synthesis of hopeahainol A (**3**).

According to our latest strategy for the total synthesis of hopeahainol A (**3**), the next objective was to forge the seven-membered carbocycle, this time relying on the premise that the conformationally more restricted substrate **58** (by virtue of the presence of the γ-lactone moiety, Scheme 7) would prove beneficial. Furthermore, given the functionalities present in the natural product, we focused our attention on the $C_{7a}-C_{8a}$ epoxide, since its anticipated intramolecular Friedel−Crafts-type opening (from C_{10b}) would form the ideal structural motifs around the $C_{7a}-C_{8a}$ bond for further elaboration. Thus, as shown in Scheme 7, epoxidation of olefinic lactone **58** with *m*-CPBA furnished epoxide **59** (∼1:1 dr). The Lewis acid-induced ring closure of epoxide **59** was next investigated, and the results are listed in Table 2. Of the conditions employed, those involving $SnCl_4$ in CH_2Cl_2 at −60 → −30 °C proved the highest yielding (62%), and led to the two diastereomeric cyclized products **63** (major) and **62** (minor) in ∼2:1 ratio (entry 1). Similar results were obtained under the promoting influence of $BF_3 \cdot Et_2O$ (entry 2, 58% yield) and $ZnCl_2$ (entry 3, 53% yield). $TiCl_4$ (entry 4, 37% yield), $CeCl_3$ (entry 5, 34% yield), and Me_2AlCl (entry 6, 30% yield) gave lower yields of the now exclusively formed diastereoisomer **63**. The structure of the major isomer (**63**, mp = 230−231 °C from CH_2Cl_2/hexane) was determined through X-ray crystallographic analysis (see ORTEP, Figure 4).[16] It was interesting to note that the diastereoisomeric ratio (dr) of the starting epoxides **59** (∼1:1) did not faithfully translate into the dr of the products **63** and **62** (∼2:1 or higher) in these experiments. To rationalize these observations, we propose that

Scheme 7. Synthesis of Hexacyclic Hydroxy γ-Lactones **62** and **63**[a]

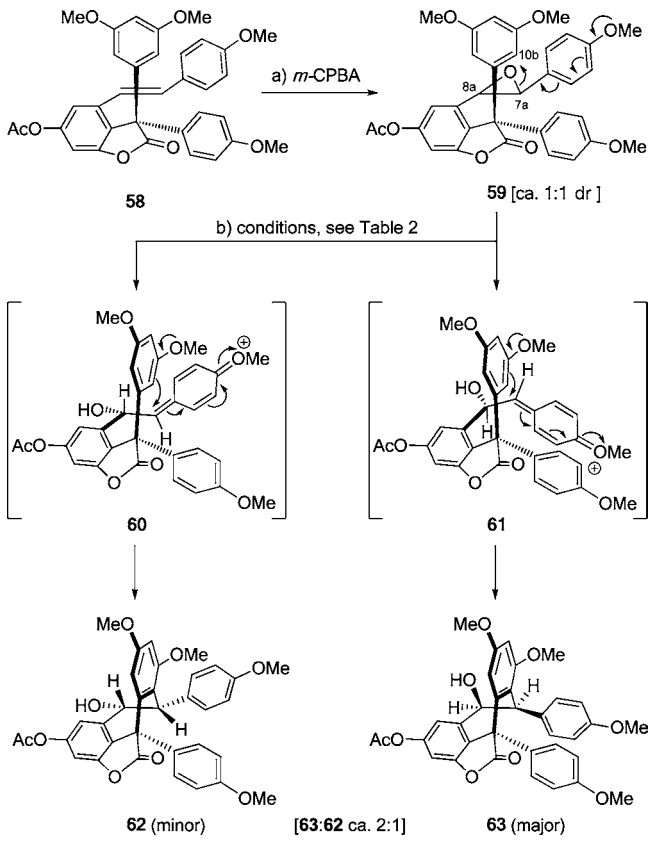

[a] Reagents and conditions: (a) *m*-CPBA (77 wt %/wt, 4.0 equiv), $NaHCO_3$ (6.0 equiv), CH_2Cl_2, 0 °C, 0.5 h, (~1:1 mixture of diastereoisomers); (b) see Table 2.

Table 2. Intramolecular Friedel–Crafts Reaction of Epoxide **59** (~1:1 dr) Leading to Hexacyclic Hydroxy γ-Lactones **62** and **63**[a]

entry	promoter, conditions	yield (%)[b]	**63**:**62** (ratio)
1	$SnCl_4$, −60 → −30 °C, 1 h	62	~2:1
2	$BF_3 \cdot Et_2O$, −78 → −50 °C, 1 h	58	~2:1
3	$ZnCl_2$, 0 → 23 °C, 8 h	53	~2:1
4	$TiCl_4$, −78 → −50 °C, 1 h	37	**63** only
5	$CeCl_3$, 0 → 23 °C, 12 h	34	**63** only
6	Me_2AlCl, 0 → 23 °C, 3 h	30	**63** only

[a] Reactions were carried out using 1.5 equiv of promoter in CH_2Cl_2. [b] Yields refer to chromatographically and spectroscopically homogeneous materials for the two steps from **58**.

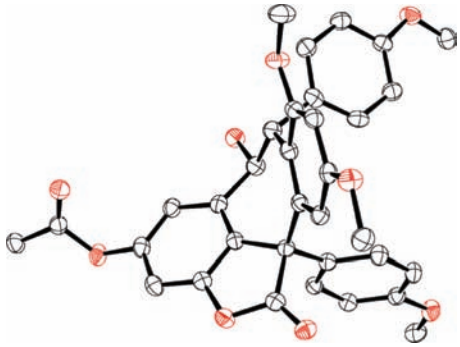

Figure 4. X-ray derived ORTEP of hexacyclic hydroxy γ-lactone **63** with thermal ellipsoids shown at the 50% probability level.[16]

the diastereoisomeric transition states **61** and **60** have different reactivity profiles, with the latter having the propensity to undergo undesirable reaction pathways. Since both C_{7a} and C_{8a} carbons in the target molecule (hopeahainol A) are sp^2-hydridized (*p*-quinonemethide and carbonyl), it seemed logical that neither the epoxidation nor the cyclization diastereoselectivity outcome in this sequence is of stereochemical consequence. However, as we shall see later, stereoselectivity at this stage has important downstream consequences which arise from drastically different reactivities of the two diastereoisomeric alcohols (**62** and **63**).

The final stages of the total synthesis of (−)-hopeahainol A [(−)-**3**)] and (−)-hopeanol [(−)-**2**)], as summarized in Scheme 8, proved interesting despite the presumption that all that was required to convert the mixture of hydroxy lactones **62**/**63** to (−)-hopeahainol A [(−)-**3**)] was oxidation and deprotection. To this end, oxidation conditions were sought first. Table 3 summarizes the results of this investigation that led to the adoption of IBX as the preferred oxidant (entry 1). Indeed, treatment of **62**/**63** (~1:2 dr) with IBX in DMSO at ambient temperature for 24 h led to ketone *p*-quinonemethide **66** (66% yield) and ketone **64** (26% yield), the former apparently formed from ketone **65** whose oxidation proved facile under the reaction conditions. In contrast, its C_{7a} diastereoisomeric ketone **64** proved intransigent to oxidation, not only under these conditions but also under a variety of other protocols including those listed in Table 3. These conclusions were based on oxidation experiments (IBX) using pure diastereoisomers **62** and **63** and their partially oxidized counterparts **64** and **65**. Attempts to epimerize ketone **64** to its oxidizable epimer **65** under a variety of conditions (e.g., LDA, KO*t*-Bu, DBU, KHMDS, NaOMe) failed. From the practical point of view, the desired ketone *p*-quinonemethide **66** was obtained through the IBX oxidation of the mixture **62**/**63**, followed by chromatographic separation, which removed the intransigent ketone **64**. Removal of the acetate group from **66** was then achieved under mild conditions ($NaHCO_3$, MeOH) to afford phenol **67** in quantitative yield. Before moving forward with the synthesis, the latter intermediate was methylated (K_2CO_3, MeI, 90% yield) to afford *ent*-tetramethyl hopeahainol A (**68**), the ^1H NMR spectrum (acetone-d_6, −30 °C) of which exhibited identical signals to those reported for permethylated natural hopeahainol A.[10] Having confirmed, through this exercise, the skeletal identity of intermediate **67** to that of hopeahainol A (**3**), all that remained for us to accomplish before arriving at the latter was its complete demethylation. This was conveniently performed under the influence of BBr_3 in CH_2Cl_2 at −78 → −20 °C, conditions that led initially to a labile intermediate, presumed to be **69** (likely X = Br or OH), whose exposure to SiO_2 led to its collapse to (−)-hopeahainol A [(−)-**3**)] in 84% overall yield. The projected conversion of (−)-hopeahainol A [(−)-**3**)] to (−)-hopeanol [(−)-**2**)] was realized by careful treatment of the former with one equivalent of NaOMe in MeOH, presumably through the intermediacy of methyl ester **70** resulting from methanolysis of the γ-lactone moiety. Indeed, it is presumed that the latter event is essential for the final carbon–carbon bond (C_{7a}–C_{1b})-forming reaction to occur, since the lactone ring imposes prohibitive conformational constraints on the hopeahainol A structure (distance between C_{7a} and C_{1b} too long, manual molecular modeling) for it to undergo the desired skeletal

(16) CCDC-770505 contains the supplementary crystallographic data for compound **63**. This data can be obtained free of charge from The Cambridge Crystallographic Data Centre via www.ccdc.cam.ac.uk/data_request/cif.

Scheme 8. Completion of the Total Synthesis of (−)-Hopeanol [(−)-**2**)] and (−)-Hopeahainol A [(−)-**3**)][a]

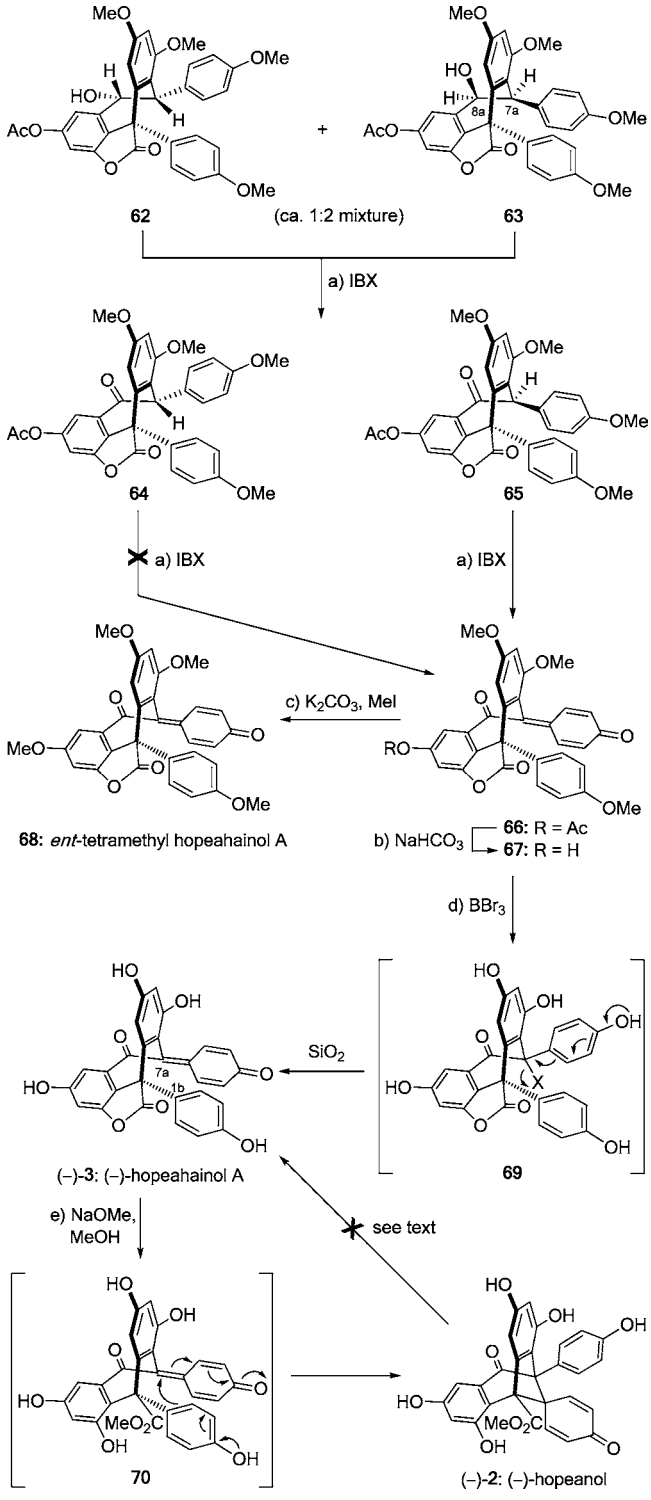

[a] Reagents and conditions: (a) IBX (10.0 equiv), DMSO, 23 °C, 24 h, **66**: 66%, plus **64**: 26%; (b) $NaHCO_3$ (sat. aq)/MeOH (1:3), 25 °C, 1 h, 100%; (c) MeI (20 equiv), K_2CO_3 (5.0 equiv), acetone, 80 °C, 1 h, 90%; (d) BBr_3 (1.0 M in CH_2Cl_2, 18 equiv), CH_2Cl_2, −78 → −20 °C, 24 h; then SiO_2, 84%; (f) NaOMe (1.0 equiv), MeOH, 25 °C, 60 h, 80%. IBX = 2-iodoxybenzoic acid; DMSO = dimethylsulfoxide.

rearrangement. The spectral data (^1H and ^{13}C NMR spectroscopic and mass spectrometric data) for synthetic (−)-**2** and (−)-**3** matched those reported for natural hopeanol and hopeahainol A.[9,10] As expected, the synthetic compounds exhibited opposite optical rotations to those reported for the naturally occurring materials.[9,10]

Table 3. Oxidation Studies of Alcohols **62** and **63**[a]

entry	oxidant, conditions	products **64**:**65**:**66** yields (%)[b]
1	IBX, DMSO	26:0:66
2	DMP, $NaHCO_3$ (20 equiv), CH_2Cl_2	14:32:33
3	PCC, CH_2Cl_2	15:0:34
4	SO_3·py, Et_3N (20 equiv), DMSO/CH_2Cl_2 (1:5)	0:0:0[c]
5	DDQ, MeCN	0:0:0[d]
6	CAN, MeCN	15:0:0[c]

[a] Reactions were carried out under the following conditions: **62**+**63** (17 μmol, ∼1:2 mixture of diastereoisomers), oxidant (10.0 equiv), 23 °C, 24 h. [b] Yields refer to chromatographically and spectroscopically homogeneous materials. [c] Starting material fully consumed. [d] 70% recovered starting material.

Our attempts thus far to confirm the proposed biosynthetic hypothesis[10] postulating hopeanol (**2**) as the precursor of hopeahainol A (**3**) failed, despite the employment of a plethora of basic and nucleophilic conditions [e.g., LiOH, LiOOH, NaOH, $Ba(OH)_2$, KO*t*-Bu, LiI/py, TMSOK, EtSNa].

The above sequence leading from γ-lactone **58** (Scheme 7) to (−)-hopeahainol A [(−)-**3**)] and (−)-hopeanol [(−)-**2**)] also served to synthesize the naturally occurring forms of these natural products from γ-lactone *ent*-**58** (Scheme 6). Synthetic (+)-hopeahainol A [(+)-**3**)] and (+)-hopeanol [(+)-**2**)] exhibited physical properties identical to those of the natural substances, and closely matching optical rotations.[9,10,17] In addition, we prepared *ent*-**46** by using the antipodal CBS catalyst in Scheme 5 and employed it to enrich our supplies of *ent*-**58** (see Supporting Information for schemes and experimental details for these two sequences).

Biological Evaluation of Synthesized Compounds. The synthesized compounds [(±)-**2**, (−)-**2**, (+)-**2**, (±)-**3**, (−)-**3**, (+)-**3**] were tested against a panel of cancer cells, including breast (MCF-7), lung (NCI-H460), CNS (SF268), nasopharyngeal (KB), and cervical (HeLa) cells using doxorubicin, Taxol®, and 5-fluorouracil as standards; the results are summarized in Table 4. Whereas the absence of significant cytotoxicity for the hopeahainols [(±)-**3**, (−)-**3** and (+)-**3**] (entries 4, 5, and 6, respectively)] was not surprising (given the isolation reports),[9,10] it was for the hopeanols [(±)-**2**, (−)-**2** and (+)-**2**] (entries 7, 8, and 9, respectively)]. Thus, and in stark contrast to the previous reports [IC_{50} = 0.52 μM against KB cell line and IC_{50} = 3.21 μM against Hela cell line for (−)-**2**],[9] racemic [(±)-**2**] and enantiomerically pure [(−)-**2** and (+)-**2**] hopeanols failed to demonstrate strong cytotoxicity against the cell lines tested. Interestingly, however, the unnatural enantiomer of hopeanol [(−)-**2**] exhibited higher potencies than the natural enantiomer [(+)-**2**] (see entry 9, Table 4).

On the other hand, acetylcholinesterase inhibition studies (see Table 5) with synthetic hopeahainols [(±)-**3**, (−)-**3**, and (+)-**3**] and hopeanols [(±)-**2**, (−)-**2**, and (+)-**2**] confirmed the previously reported results with hopeahainol A [(+)-**3**] (entry 5, IC_{50} = 3.63−4.92 μM, lit.[10] IC_{50} = 4.33 μM). All the other tested

(17) While the optical rotation of synthetic (+)-hopeahainol A [(+)-**3**] was in close agreement to that reported in the literature [$[\alpha]_D^{25}$ = +650.0 [MeOH, *c* = 0.075; lit.: $[\alpha]_D^{25}$ = +673.5 (MeOH, *c* = 0.09)]],[10] that of synthetic (+)-hopeanol [(+)-**2**], although it showed the same sign, differed significantly in absolute value to that reported in the literature [$[\alpha]_D^{25}$ = +193.0 (MeOH, *c* = 0.070); lit.: $[\alpha]_D^{25}$ = +40.1 (MeOH, *c* = 0.23)]].[9]

Table 4. Cytotoxicity of Synthetic Racemic and Enantiomerically Pure Hopeanols [(±)-**2**, (−)-**2**, and (+)-**2**] and Hopeahainols [(±)-**3**, (−)-**3**, and (+)-**3**] Against Selected Cancer Cell Lines (GI_{50} values in μM)[a]

		cell line				
entry	compound	MCF-7[b]	NCI-H460[b]	SF268[b]	KB[c]	HeLa[c]
1	doxorubicin	0.085 ± 0.009	0.052 ± 0.009	0.481 ± 0.019	0.201 ± 0.082	0.094 ± 0.004
2	Taxol®	0.007 ± 0.001	0.007 ± 0.001	0.030 ± 0.009	0.007 ± 0.001	0.008 ± 0.001
3	5-fluorouracil	6.42 ± 0.50	6.38 ± 0.42	66.14 ± 17.12	71.55 ± 5.88	8.06 ± 0.76
4	(±)-**3**	88.45	>100	>100	>100	>100
5	(−)-**3**	64.00 ± 2.02	63.29 ± 5.19	65.79 ± 0.26	72.43 ± 12.81	>100
6	(+)-**3**	99.05 ± 8.34	>100	>100	>100	>100
7	(±)-**2**	>100	>100	>100	>100	>100
8	(−)-**2**	89.56 ± 13.24	76.44 ± 4.74	>100	>100	>100
9	(+)-**2**	28.04 ± 1.30	32.69 ± 8.13	29.22 ± 6.42	33.19 ± 11.05	25.71 ± 5.62

[a] Antiproliferative effects of tested compounds against human tumor cell lines and drug-resistant cell lines in a 48 h growth inhibition assay using the sulphorhodamine B staining methods. Human cancer cell lines: breast (MCF-7), lung (NCI-H460), CNS (SF268), nasopharyngeal (KB) and cervical (HeLa). Growth inhibition of 50% (GI_{50}) is calculated as the drug concentration which caused a 50% reduction in the net protein increase in control cells during drug incubation. GI_{50} values for each compound are given in μM and represent the mean of 1−4 independent experiments ± standard error of the mean. [b] These cell lines were provided by the National Cancer Institute (NCI), Division of Cancer Treatment and Diagnosis (DCTD). [c] These cell lines were provided by ATCC.

Table 5. Inhibition of Acetylcholinesterase Activity by Synthetic Racemic and Enantiomerically Pure Hopeanols [(±)-**2**, (−)-**2**, and (+)-**2**] and Hopeahainols [(±)-**3**, (−)-**3**, and (+)-**3**] (IC_{50} values in μM)[a]

		time (min)					
entry	compound	10	20	30	40	50	60
1	galanthamine	0.173 ± 0.092	0.249 ± 0.089	0.270 ± 0.077	0.278 ± 0.063	0.338 ± 0.048	0.373 ± 0.033
2	huperzine	0.036 ± 0.016	0.035 ± 0.007	0.034 ± 0.005	0.033 ± 0.005	0.033 ± 0.004	0.034 ± 0.003
3	(±)-**3**	>50	>50	>50	>50	>50	>50
4	(−)-**3**	>50	>50	>50	>50	>50	>50
5	(+)-**3**	4.92 ± 0.09	4.78 ± 1.07	3.67 ± 0.39	3.63 ± 0.03	3.82 ± 0.09	3.96 ± 0.25
6	(±)-**2**	>50	>50	>50	>50	>50	>50
7	(−)-**2**	>50	>50	>50	>50	>50	>50
8	(+)-**2**	>50	>50	>50	>50	>50	>50

[a] Acetylcholinesterase inhibitory activities of tested compounds in kinetic-based experiments using Ellman's method. Inhibition of 50% (IC_{50}) of acetylcholinesterase activity is calculated as the drug concentration which caused a 50% reduction in the enzyme activity as compared to that with a negative control. IC_{50} values for each compound are given in μM and represent the mean of 2−5 independent experiments ±standard error of the mean.

compounds failed to exhibit any inhibitory activity in this assay at below 50 μM concentrations.

Conclusion

The chemistry described herein demonstrates the power of cascade reactions in complex molecule construction[12] and provides access to (+)-hopeanol [(+)-**2**] and (+)-hopeahainol A [(+)-**3**], two structurally intriguing resveratrol-derived natural products. While our biological studies with synthetic material confirmed the reported acetylcholinesterase inhibitory activity of hopeahainol A, they failed to reveal the reported cytotoxicity potency for hopeanol. The latter discrepancy may be due to contaminant(s) of the natural product or a variation of the biological assays employed. We have also failed to produce experimental evidence for the proposed biosynthetic step that would implicate hopeanol as the precursor to hopeahainol A.[10] On the contrary, we realized the reverse transformation whereby hopeahainol A was smoothly converted to hopeanol under alkaline methanolic conditions. The reported synthetic strategies and technologies are expected to facilitate further developments, including the design, synthesis, and biological evaluation of related compounds as potential tools and drug candidates for the treatment of diseases such as cancer and Alzheimer's.

Acknowledgment. Professor K. C. Nicolaou is also at the Department of Chemistry and The Skaggs Institute for Chemical Biology, The Scripps Research Institute, 10550 North Torrey Pines Road, La Jolla, California 92037 (U.S.A.), and the Department of Chemistry and Biochemistry, University of California, San Diego, 9500 Gilman Drive, La Jolla, California 92093 (U.S.A.). We thank Mr. Rong-Ji Sum (CSL-ICES) for his assistance in the biological studies, Dr. Aitipamula Srinivasulu (ICES) and Ms. Chia Sze Chen (ICES) for X-ray crystallographic analysis, and Ms. Doris Tan (ICES) for high-resolution mass spectrometric (HRMS) assistance. Financial support for this work was provided by A*STAR, Singapore.

Supporting Information Available: Experimental procedures, and compound characterization. This material is available free of charge via the Internet at http://pubs.acs.org.

JA102623J